

THE AFFECTS OF ORGANIC AND INORGANIC NITROGEN LOADING ON MICROPLANKTON TROPHIC STRUCTURE: A MICROCOSM EXPERIMENT

Noam Ross, Center for Environmental Studies, Brown University

Charles Hopkinson, The Ecosystems Center, The Marine Biological Laboratory

A Semester in Environmental Studies Project, Fall 2004

Introduction

Bacteria and phytoplankton form the base of the pelagic food web. Due to size differences within and across these groups, as well as nutrient and energy content, the balance of bacteria and phytoplankton affects higher trophic levels (Azam et. al. 1983). Balance of phytoplankton and bacteria also control the net respiration of the pelagic system – phytoplankton are the main primary producers and bacteria account for most of respiration (Hopkinson et. al. 1989).

Phytoplankton use inorganic nutrients and carbon for production, while bacteria use organic matter. Production by both is related by the fact that phytoplankton can release dissolved organic matter, bacteria re-mineralize organic matter, and bacteria can take up inorganic nutrients when organic nutrients are limiting.

Land use changes by humans modify the inputs of both inorganic nitrogen and organic matter to estuaries (Hopkinson and Vallino 1995). Therefore, land use change can affect bacterial/phytoplankton balance and thus higher trophic levels and net ecosystem respiration and production.

I studied how to different types of nitrogen loading affect production of phytoplankton, bacteria, and heterotrophic nanoflagellates that act as food sources for macrozooplankton. I incubated a marine microplankton community in microcosms under high concentrations of DIN and DON and measured the biomass, production, and size distribution of phytoplankton, bacteria, and nanoflagellates in order to quantify flow of carbon through these pelagic organisms to higher trophic levels.

I hypothesized that under conditions of DIN loading, phytoplankton production will drive the microplankton trophic structure and both phytoplankton and zooplankton of larger size classes will dominate. Under DON loading, bacterial production will drive phytoplankton trophic structure and smaller size classes of both phytoplankton and zooplankton will dominate.

Methods

Four 18-l Bellco[®] glass bioreactors were incubated in Conviron[®] PGR-15 growth chambers at 20°C under a cycle of 12 hours light and 12 hours darkness. Light was provided by both halogen and fluorescent bulbs and levels were $2000 \pm 25 \mu\text{E}/\text{cm}^2$ during

the light phase. The microcosms were stirred constantly at 20 RPM using Bellco[®] overhead drives..

All microcosms were filled with 9 liters seawater from Woods Hole Harbor (~32 ppt), that had been gravity-filtered through 150-nm Nytex mesh. Two microcosms were augmented with 2 liters of nitrate-loaded artificial seawater. The artificial seawater contained 32 ppt Instant Ocean[®] sea salts, 200 μM KNO_3 , 290 μM Na_2SiO_3 , and 20 μM KH_2PO_4 . To the other two microcosms, 9 liters of DOM-rich water were added. DOM rich water was collected from Hidden Swamp in Woods Hole, MA. 32 ppt of Instant Ocean[®] sea salts were added to the swamp water and it was stored for 48 hr at 40°C to allow for flocculation. After 48 hr, the swamp water was pressure-filtered to remove all particulate matter >1 μm . 290 μM Na_2SiO_3 and 20 μM KH_2PO_4 were then added. Both nutrient additions were raised to pH 8 using NaOH prior to mixing with seawater. At time of addition to the microcosms, the DOM-rich water had DOC concentration of 7400 μM and DON concentrations of 110 μM (C:N = 67), as well as 2.0 μM NO_3^- and 3.5 μM NH_4^+ .

3 days after addition nutrient addition, 100 ml of pure phytoplankton inoculate was added to all treatments.

Microcosms were sampled once before nutrient addition and at regular intervals for a week thereafter to measure concentrations of NH_4^+ , NO_3^- , DON, and DOC, bacterial populations, nanoflagellate populations, and Chl-a concentrations of both the <10 μm and >10 μm fractions of phytoplankton. Also measured regularly were bacterial production and gross primary production. Nitrate treatment microcosms were sampled again after two weeks to assess post-bloom conditions. Microcosm dissolved oxygen and pH were monitored continuously with Bellco[®] electronic probes. One microcosm of each treatment served as the “primary microcosm” and was sampled with greater regularity. The other served as a replicate and was sampled less often. Data reported is from the primary microcosm unless otherwise noted.

Nitrogen species concentrations were measured on water filtered through Whatman GF/F filters (0.7 μm pores size). NH_4^+ concentration were measured via the phenol-hypochlorite method from Strickland and Parsons (1972), using a Shimadzu 1601 spectrophotometer. NO_3^- concentrations were measured by reducing to NO_2^- via reaction with tetrasodium ethyl acetate with a cadmium-copper catalyst and then measured via diazotization (Wood, 1967). The process was automated on on a Lachat QuickChem 8000 flow injection analyzer. Total dissolved nitrogen was determined by converting all N to NO_3^- using the persulphate oxidation method (Valderrama 1981) and measuring NO_3^- as above.

20 ml samples were filtered through Whatman GF/F filters and stored at -10°C for DOC determination. DOC concentrations were determined via high-temperature catalytic oxidation (HTCO) following Peltzer and Brewer (1993). Samples were acidified with 10 μl 5N phosphoric acid and sparged with O_2 gas for ten minutes before combusting.

Bacterial and nanoflagellate numbers were determined from glutaraldehyde-fixed samples stained with DAPI to a final concentration of 10 mg/l (Porter and Feig 1980). For bacteria, 0.2 to milliliters of sample were filtered onto black 0.2- μm Millipore filters.

For nanoflagellates, 2 to 4 milliliters of sample were filtered onto black 0.8- μm Millipore filters. A Zeiss standard microscope with a 100 \times objective was used for counting. At least 20 10,000- μm^2 fields or 1000 cells were counted in each sample. Only heterotrophic nanoflagellates were counted by eliminating organisms that showed chlorophyll autofluorescence.

Chlorophyll concentrations were determined spectrophotometrically following Lorenzen (1967) on a Perkin Elmer Lambda Bio-20 spectrometer. 500-ml water samples were filtered successively onto 10 μm Nytex mesh and then onto Whatman GF/F filters. Chlorophyll was then extracted from the filters with 90% acetone at -10°C in the dark for 48 hr, and absorbance at 665 nm was determined after centrifugation to remove particles. Phaeopigment concentrations were also measured by acidifying samples. Filters were stored at -10°C for up to two weeks prior to acetone extraction.

Bacterial production was measured via uptake of ^{14}C -labeled leucine (Simon and Azam, 1989). ^{14}C -leucine (350 Ci/mol) was added to 2 ml sample to a final concentration of 3×10^{-10} M. Samples were incubated at room temperature for 1 hour. Incubation was terminated with the addition of 0.2 ml 50% trichloroacetic acid (TCA). TCA was added to control samples prior to incubation to determine abiotic uptake of leucine. Samples were filtered onto 0.2 μm nitrocellulose filters using 5% TCA to precipitate protein. Filters were placed in scintillation vials and dissolved using Cellusolve[®]. Radiation was measured using a scintillation counter and 30% Scintisafe scintillation fluid.

Gross primary production of both total phytoplankton and the >10 μm fraction was measured via uptake of ^{14}C -bicarbonate. 5 μCi of H^{14}CO_3 (57.0 Ci/mol) in 1 ml was added to 60-ml water samples in glass BOD bottles and incubated under the same conditions as the microcosms for 4 hours. Incubation was terminated by placing bottles in a dark box. Control samples were incubated in the dark to determine dark-process CO_3 uptake. Samples were filtered onto both 10 μm Nytex screen and 0.2 μm nitrocellulose filters. Filtrate from 0.2 μm filters was retained to determine DOC production. Samples were acidified using 5.5 N HCl and placed in a chemical hood for 24 hours to de-gas. Radiation was then measured on a scintillation counter and 30% Scintisafe scintillation fluid.

To convert measured value to carbon stocks and flows in microplankton, the following conversions were used: Bacteria were assumed to contain 25 fg C/cell (Fukuda et. al. 1998). Nanoflagellates were assumed to be spherical in shape and contain 183 fg C/ μm^3 . A C:Chl-a ratio of 50 was used (Caron et. al. 1995). Bacterial carbon production was calculated from leucine uptake rates assuming 100% incorporation of leucine, that leucine made up 7.3% of bacterial protein by weight, protein made up 63% of bacterial dry weight, and 54% of bacterial dry weight was carbon (Simon and Azam 1989). Gross primary production was calculated from ^{14}C -bicarbonate uptake assuming 2.0 mM DIC in seawater.

Results

Prior to nutrient addition, seawater in all microcosms contained $0.9 \pm 0.3 \mu\text{M}$ NH_4^+ , $0.0 \pm 0.1 \mu\text{M}$ NO_3^- , and $11.6 \pm 1.3 \mu\text{M}$ DON. DOC concentrations were $162 \pm 8.7 \mu\text{M}$. (C:N = 14). Bacterial populations were 2.5×10^6 cells/ml and nanoflagellates were 1.6×10^3 cells/ml. Chlorophyll concentrations were $3.4 \pm 0.1 \mu\text{g/l}$, with 47% of the chlorophyll in phytoplankton under $>10 \mu\text{m}$. Bacterial production was $0 \pm 1 \mu\text{g C/l-hr}$. Daytime gross primary production was $33 \pm 30 \mu\text{g C/l-hr}$, with 30% of the production occurring in the $>10 \mu\text{m}$ fraction. DOC production was $0.7 \mu\text{g/l-hr}$.

NH_4^+ concentrations were low in all treatments for the duration of the experiment (Figure 1). In the swampwater treatment, NO_3^- concentrations remained low for the entire experiment. DON declined from 48 to $35 \mu\text{M}$ over the first 3 days of the experiment and remained constant thereafter. In the nitrate treatment, NO_3^- concentrations remained high, at $80 \mu\text{M}$, for the first week, though at the end of the second week they had declined to $0.2 \mu\text{M}$. Due to noise in the NO_3^- data, I was unable to determine DON concentrations for the nitrate treatment. Nitrogen dynamics replicated well for all species in both treatments.

DOC concentrations were approximately 40 times higher in the swampwater treatment than the nitrate treatment (Figure 2). DOC concentrations declined in both treatments over the first week. In the swampwater treatment, $49 \mu\text{g/l-hr}$ DOC was lost over the week. Flocculation of organic matter was observed in this microcosm and may have contributed to DOC loss. In the nitrate treatment, $3.4 \mu\text{g/l-hr}$ was lost. After the second week, DOC in the nitrate treatment rose to $765 \mu\text{M}$. DOC increase from inoculation to the end of the second week was $32 \mu\text{g/l-hr}$.

Bacteria population grew tenfold in the swampwater treatment in the first three days of the experiment, then crashed over the course of one day and remained relatively steady afterwards (Figure 3). Bacterial carbon increase during the bloom was $10 \mu\text{g/l-hr}$, over the course of the cycle it was $2 \mu\text{g/l-hr}$. Nanoflagellate population remained low in the swampwater treatment until bacterial population peaked, after which the nanoflagellate population rose rapidly over the course of a day. Nanoflagellate population declined steadily from day four to the end of the experiment. Nanoflagellate population was related to bacterial population 40 hours previous ($R^2 = 0.79$). Nanoflagellate carbon increased $19 \mu\text{g/l-hr}$ during the bloom, but $0 \mu\text{g/l}$ over the course of the cycle. Peak nanoflagellate population corresponded with the crash of bacterial population. In the nitrate treatment, bacterial and nanoflagellate populations remained steady for the first week. After two weeks, bacterial population remained the same and nanoflagellate population had risen to 0.05 million cells/ml. From inoculation to the end of the second week, Increase in bacterial carbon was $0 \mu\text{g/l-hr}$, increase in nanoflagellate carbon was $1 \mu\text{g/l-hr}$.

Bacterial production declined slightly in the swampwater treatment over the course of the first week, while in the nitrate treatment they remained steady at approximately $1 \mu\text{g/l-hr}$. (Figure 4). Overall, bacterial production was 30X greater in the swampwater treatment than the nitrate treatment in the first week. However, bacterial production increased to $20 \mu\text{g/l-hr}$ at the end of the second week in the nitrate treatment. Bacterial production averaged $32 \mu\text{g/l-hr}$ in the swampwater treatment over the first week, and averaged $10 \mu\text{g/l-hr}$ in the nitrate treatment from inoculation to the end of the second week.

Chl-a concentrations were approximately twice as high in the swampwater treatment than in the nitrate experiment over the first week (Figure 5). In both treatments, concentrations were steady over the first three days then rose following the addition of the phytoplankton inoculate. In both treatments, $55 \pm 10\%$ of the Chl-a was in phytoplankton greater than $10 \mu\text{m}$ over the course of the week. In the swampwater treatment, Chl-a concentrations peaked at six days and change in phytoplankton carbon was $2.4 \mu\text{g/l}\cdot\text{hr}$. After two weeks, Chl-a in the nitrate treatment had risen sixtyfold to $86 \mu\text{g/l}$, and 84% of it was in phytoplankton greater than $10 \mu\text{m}$. Phytoplankton carbon increased $17 \mu\text{g/l}\cdot\text{hr}$ from inoculation to the end of the second week. Chlorophyll dynamics replicated well in both treatments prior to addition of inoculate, but replicates diverged from primary treatments slightly following inoculation.

Daytime gross primary production increased in both treatments over the course of the first week, particularly after the addition of the phytoplankton inoculate (Figure X). Prior to inoculation, there was no gross primary production in the nitrate treatment. At the end of the second week, GPP in the nitrate treatment was $1130 \mu\text{g/l}\cdot\text{hr}$. Average daily GPP in the swampwater treatment in the first week was $16 \mu\text{g/l}\cdot\text{hr}$. Average daily GPP in the nitrate treatment from inoculation to the end of the second week was $240 \mu\text{g/l}\cdot\text{hr}$. Average daily DOC production in the swampwater treatment in the first week was $0.3 \mu\text{g/l}\cdot\text{hr}$. In the nitrate treatment, daily DOC production was zero for most of the first week but rose to $0.5 \mu\text{g/l}\cdot\text{hr}$ the second week.

Discussion

Figure 7 shows the flow of carbon in swampwater treatment microcosm over the course of the first week. To calculate phytoplankton respiration, I assumed that phytoplankton respiration was 37% of GPP based on oxygen concentration data from the replicate microcosm (not shown). Phytoplankton grazing rates were calculated by mass balance.

Grazing rates on bacteria by nanoflagellates were calculated by the difference between bacterial production and change in bacterial biomass. To calculate nanoflagellate respiration, I estimated nanoflagellate production efficiency. This was estimated using bacterial production and change in biomass prior to the bacterial crash, and change in nanoflagellate biomass at the corresponding time 40 hours later. At this time grazing on nanoflagellates was assumed to be negligible, and thus nanoflagellate growth efficiency was equal to change in biomass over grazing rate on bacteria. Nanoflagellate growth efficiency was calculated to be 86% . This value is high, and the actual value would be higher if grazing on nanoflagellates was significant during the bloom period. Such growth efficiencies have been reported for nanoflagellates before (Laybourn-Parry 1998). However, it is also possible that nanoflagellates are ingesting DOC directly, as has been shown to occur. (Marchant 1993).

Bacterial growth efficiency is 64% , also a very high value. This is also a minimum value as it assumes all lost DOC was consumed by bacteria, while some was lost to flocculation. Previously reported bacterial growth efficiencies on humic and

lingo-cellulose substances, which were most likely the form of most DOC in the swampwater, range from 22 to 45% (Bano 1997, Benner 1998). However, bacterial growth efficiency increases both with DOC concentrations and with exposure to high light levels (Eiler 2003, Reche 1998), both conditions which existed here. However, the calculated efficiency is likely an overestimate because of the assumption that DOC is the only carbon source. Despite efforts to minimize it, POC was present in the microcosms at the beginning of the experiment. Swampwater was filtered through 1 μm filters, but DOC samples were filtered through 0.7 μm filters. Flocculation was observed when swampwater pH was adjusted and also when it was mixed with seawater. While performing bacterial population counts, I observed large numbers of bacteria attached to POC. If bacterial growth efficiency were 29% (as calculated in nitrate treatment, see below), bacteria would be consuming at 60 $\mu\text{g C/l}\cdot\text{hr}$ of POC.

Overall, 57% of DOC consumed passes through this food chain to higher consumers, and 93% of this carbon is in the form of larger nanoflagellates. Even if both production efficiencies are off by a factor of 2, 13% of DOC consumed passes up to the next trophic level. This is a high efficiency for two trophic transfers. 60% of carbon fixed by photosynthesis available to consumers ((Change in biomass + grazing)/GPP) and 55% of this is available as large (>10 μm) phytoplankton. 26% of the total carbon available to higher consumers originated from phytoplankton production.

Figure 8 shows the carbon flow in the nitrate treatment microcosm between inoculation and the end of week two, during which time the bloom occurred. Numbers are speculative as data taken only before and after the bloom fail to capture some of the dynamics. For instance, while DOC production as measured by ^{14}C bicarbonate before and after week averaged 0.13 $\mu\text{g/l}\cdot\text{hr}$, actual change in DOC concentrations was 32 $\mu\text{g/l}\cdot\text{hr}$.

Bacterial production efficiency was calculated as 29% based on bacterial production and DOC loss in the first week, assuming no flocculation. Bacterial production was used to back-calculate DOC consumption and, using overall change in DOC, DOC production. Nanoflagellate production efficiency was assumed to be the same as in the swampwater treatment. To calculate phytoplankton respiration, I assumed that phytoplankton respiration was 35% of GPP based on oxygen concentration data from the replicate microcosm (not shown).

In this system, 22% of DOC consumed passes through the food chain to higher consumers, all of which is in the form of nanoflagellates. However, DOC in this case originates from phytoplankton, rather than swampwater DOC, so ultimately production in the heterotrophic food chain originated in the autotrophic food chain.

51% of DIC fixed by phytoplankton is available to higher consumers, a lower efficiency than in the previous treatment because more primary production went into formation of DOC. Over all, 2.5% of GPP ended up in the form of nanoflagellates, 12% in <10 μm phytoplankton, and 85% as >10 μm phytoplankton. 100% of carbon available originated from phytoplankton production. Overall amount available to higher consumers is 7.9X that available in the swampwater treatment.

In the swampwater treatment, 36 $\mu\text{g C/l-hr}$ of grazable biomass were produced for every 1 $\mu\text{g C/l-hr}$ of nitrogen that was taken up over the course of the experiment. In the nitrate treatment, 5.9 $\mu\text{g/l-hr}$ nitrogen was consumed in producing a total of 300 $\mu\text{g C/l-hr}$ grazable biomass, a ratio of 1:51. A larger difference in nitrogen use efficiency when we compare production to the nitrogen loading over the time scale of the budget. In the nitrate treatment, in which all of the nitrate was used, the loading was 5.9 $\mu\text{g/l-hr}$ nitrogen ratio remains 1:51. However, in the swampwater treatment, where less nitrogen was taken up, loading was 5.8 $\mu\text{g/l-hr}$ nitrogen and the ratio was 1:6.5.

Conclusions

This study indicates that the form in which nitrogen enters a marine pelagic system can affect how carbon flows through microplankton trophic structure by controlling the efficiency of carbon transfer, the balance of autotrophic and bacterial production and the size of phytoplankton. While these findings are limited to the spatial and temporal scales of the microcosm experiment, they suggest that the effect on marine systems of nitrogen loading can not only be predicted by the quantity of nitrogen loading but the quality of that nitrogen and the organic matter that is associated with it.

Acknowledgements

I would like to thank Charles Hopkinson, Joe Vallino and Laura Broughton for their mentorship in this project, as well as Allison Burce, Don Burnette, Ken Foreman, Sarah Foster, Hap Garritt, Bonnie Kwiatkowski, Richard McHorney, Katherine Nolan, and Ian Washbourne for logistical and psychological support.

Works Cited

- Azam, F. et. al. 1983. The Ecological Role of Water-Column Microbes in the Sea. *Marine Ecology Progress Series*, 10:257-263.
- Bano, N., Moran M.A. and R.E. Hodson. 1997. Bacterial utilization of dissolved humic substances from a freshwater swamp. *Aquatic Microbial Ecology*, 12:233-238.
- Benner, R. et. al., 1998. Carbon Conversion Efficiency for Bacterial Growth on Lignocellulose: Implications for Detritus-Based Food Webs. *Limnology and Oceanography*, 33(6):1514-1526.
- Caron D.A. et. al., 1995. The contribution of microorganisms to particulate carbon and nitrogen in surface waters of the Sargasso Sea near Bermuda. *Deep-Sea Research*, 42:943-972
- Eiler, A. et. al., 2003. Heterotrophic Bacterial Growth Efficiency and Community Structure at Different Natural Organic Carbon Concentrations. *Applied and Environmental Microbiology*, 69(7):3701-3709.

- Fukuda, R. et. al., 1998. Direct Determination of Carbon and Nitrogen Contents of Natural Bacterial Assemblages in Marine Environments. *Applied and Environmental Microbiology*. 64(9):3352-3358.
- Hopkinson, C. S. et al.. 1989. Size-Fractionated Coastal Plankton Metabolism - Substrate and Nutrient Interactions. *Marine Ecological Progress Series*, 51:155-166.
- Hopkinson, C. S., and J. J. Vallino. 1995. The Relationship among Man's Activities in Watersheds and Estuaries: A Model of Runoff Effects on Estuarine Community Metabolism. *Estuaries* 18:598-621.
- Laybourn-Parry, J. and M. Walton, 1998. Seasonal heterotrophic flagellate and bacterial plankton dynamics in a large oligotrophic lake— Loch Ness, Scotland. *Freshwater Biology*, 39(1): 1-8.
- Lorenzen, C. J., 1967. Determination of chlorophylls and phaeopigments: spectrophotometric equations. *Limnology and Oceanography* 12:343 – 346.
- Marchant, H.J. and F.J. Scott, 1993. Uptake of sub-micrometre particles and dissolved organic matter by Antarctic choanoflagellates. *Marine Ecology Progress Series*, 92:59-64
- Peltzer, E.T. and P.G. Brewer, 1993. Some practical aspects of measuring DOC – sampling artifacts and analytical problems with marine samples. *Marine Chemistry*, 41:243-252
- Porter K.G. and Y.S. Feig, 1980. The Use of DAPI for identifying and counting aquatic microflora. *Limnology and Oceanography*, 25:943-948.
- Reche, I., et. al., 1998. Interactions of Photobleaching and Inorganic Nutrients in Determining Bacterial Growth on Colored Dissolved Organic Carbon. *Microbial Ecology*, 36(3):270-280
- Simon, M. and F. Azam. 1989. Protein Content and Protein Synthesis Rates of Planktonic Marine Bacteria. *Marine Ecology Progress Series*, 51:201-213.
- Strickland, J.D.H. and T.R. Parsons. A practical handbook of Seawater Analysis. 2nd ed. Ottawa: Fisheries Research Board of Canada, 1972.
- Valderrama, J.C., 1981. The Simultaneous Analysis of Total Nitrogen and Total Phosphorous in Natural Waters. *Marine Chemistry*, 10:109-0122.
- Wood, E.D. 1967. Determination of nitrate in seawater by cadmium-copper reduction to nitrite. *Journal of the Marine Biological Association of the United Kingdom*, 47:23-31.

Figures

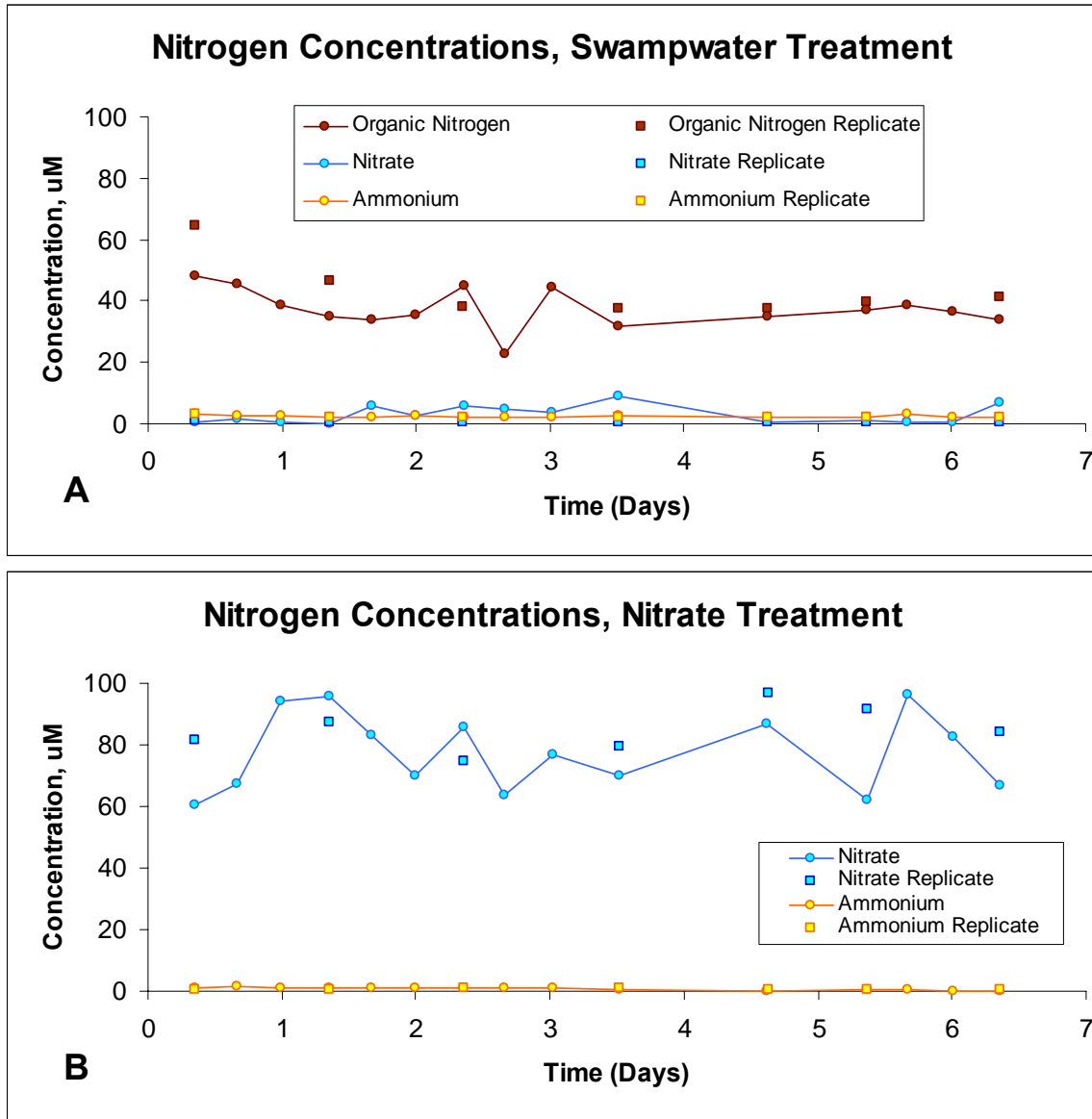


Figure 1 – Nitrogen species concentrations in microcosms. (A) Swampwater Treatment. (B) Nitrate Treatment. DON concentrations are not shown in the nutrient treatment because high variability in NO_3^- measurements made DON indistinguishable from zero.

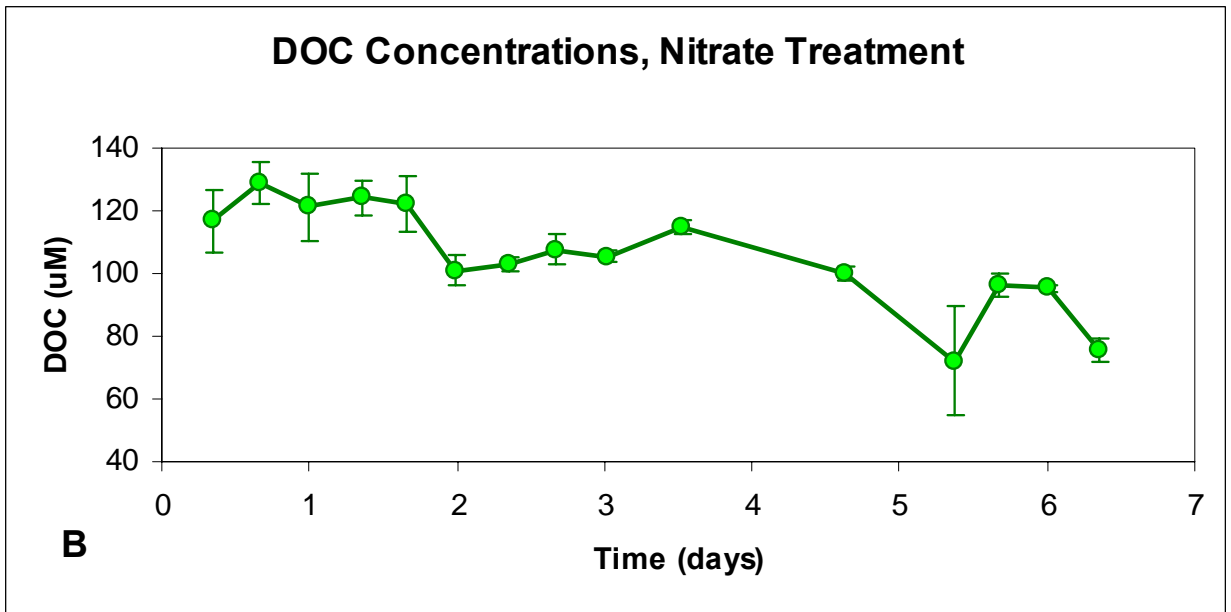
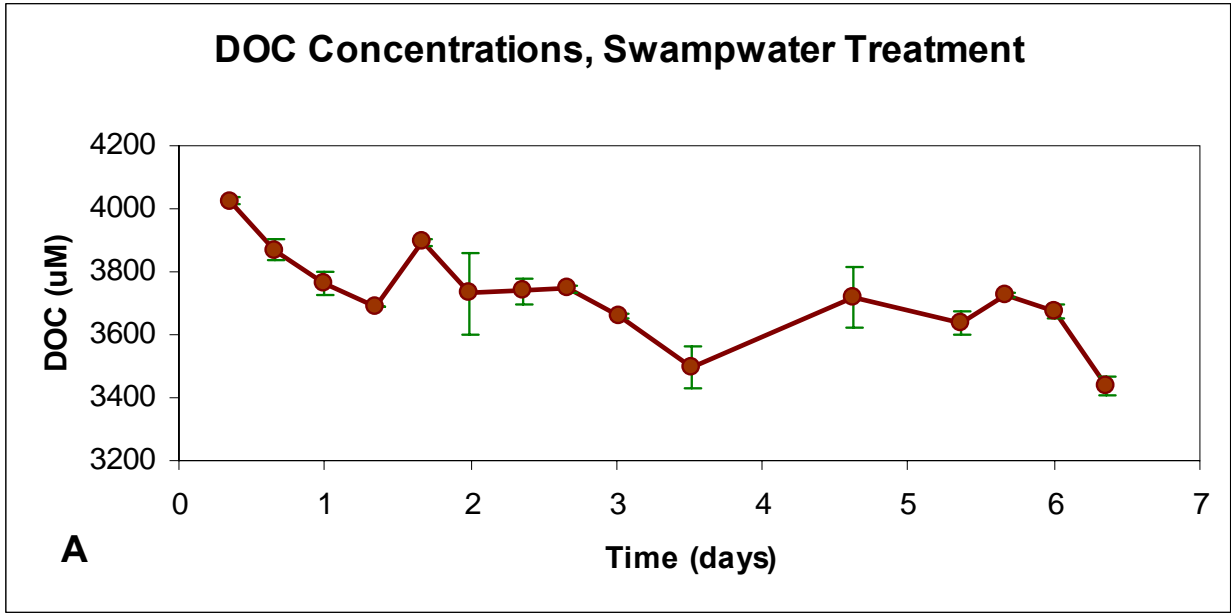


Figure 2 – DOC concentrations. (A) Swampwater Treatment. (B) Nitrate Treatment. Note differences in scale. Error bars are ± 1 standard error.

Bacteria and Nanoflagellate Populations

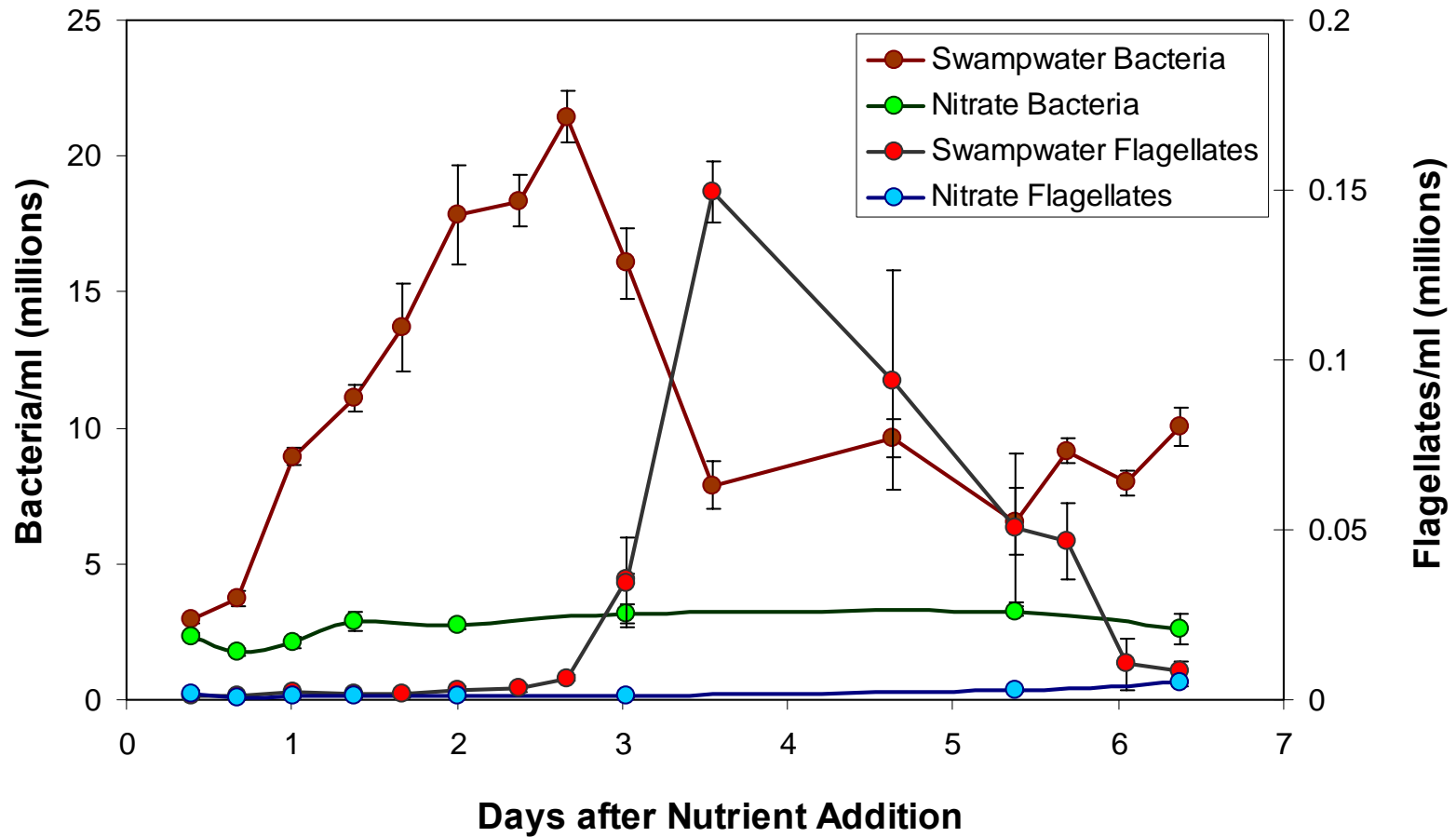


Figure 3 – Bacteria and nanoflagellate populations. Error bars are ± 1 standard error.

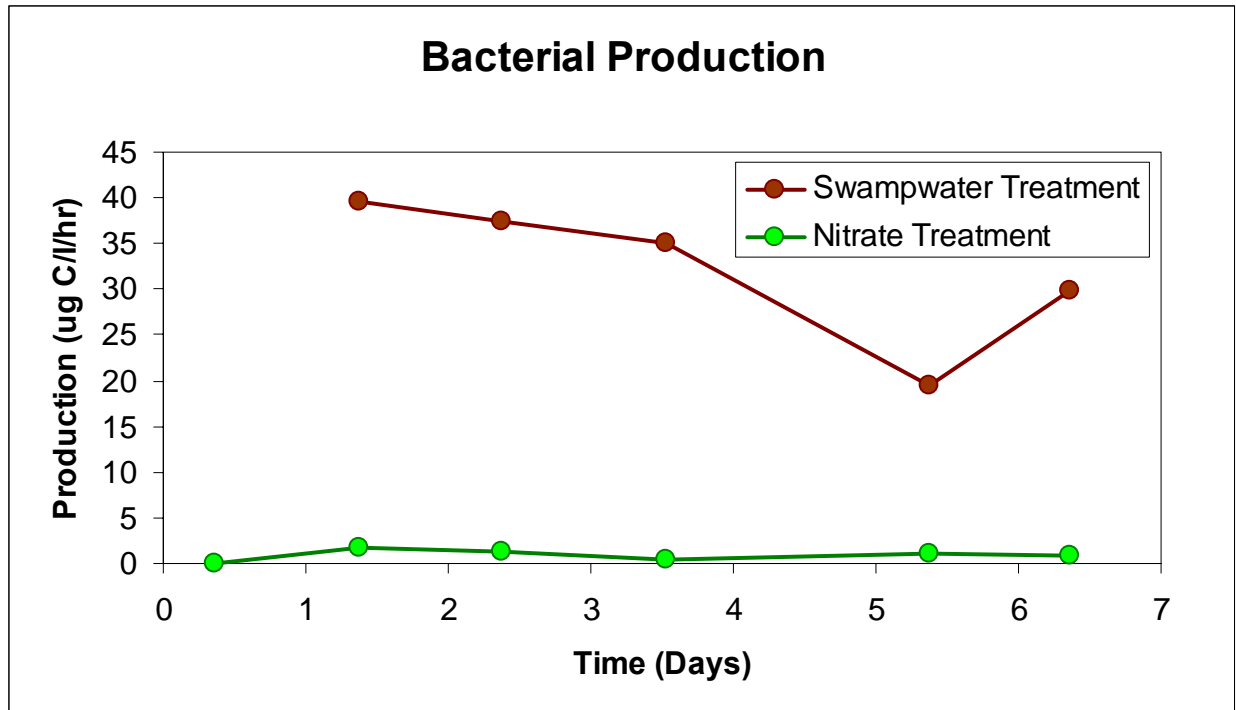


Figure 5 – Bacterial Production as measured by ^{14}C -Leucine uptake.

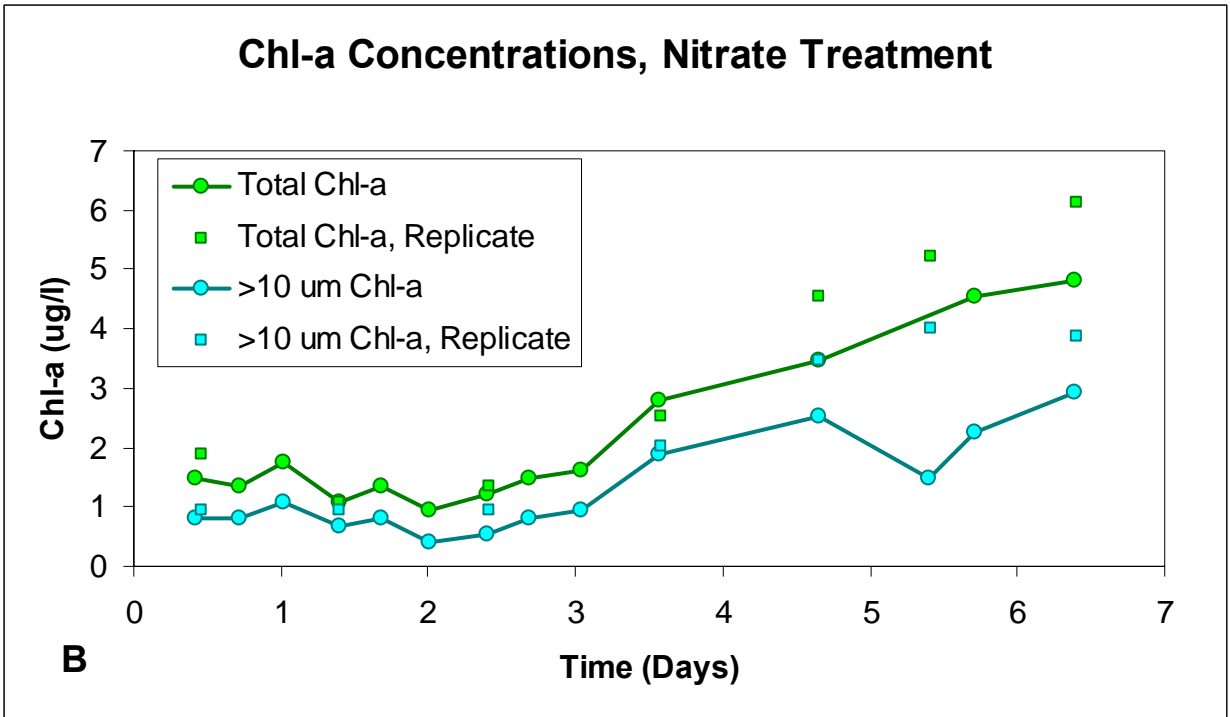
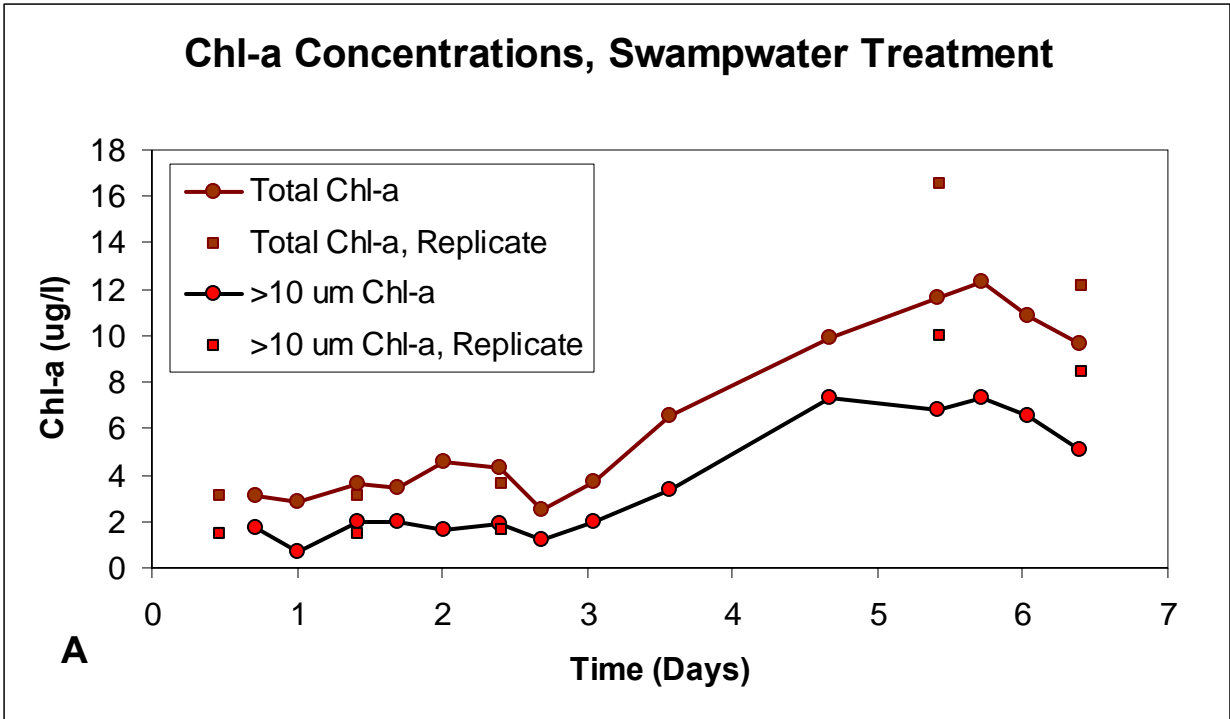


Figure 5 – Chl-a concentrations. (A) Swampwater treatment. (B) Nitrate treatment. Note differences in scale.

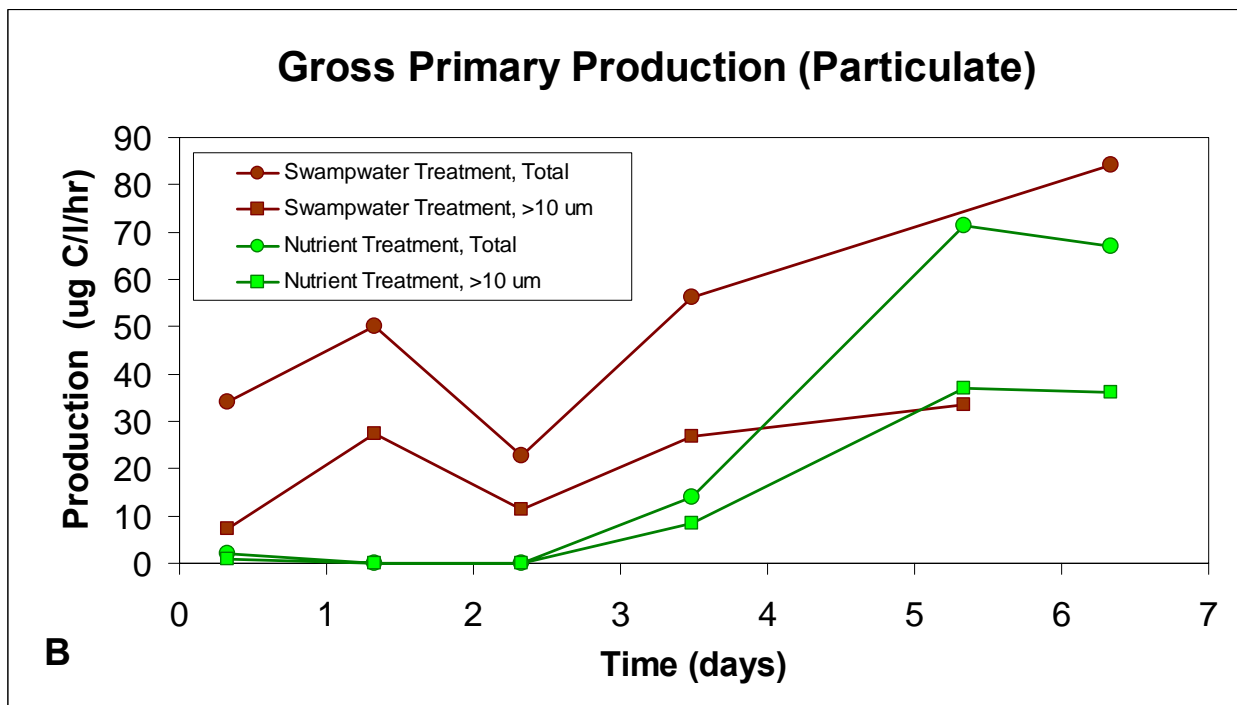
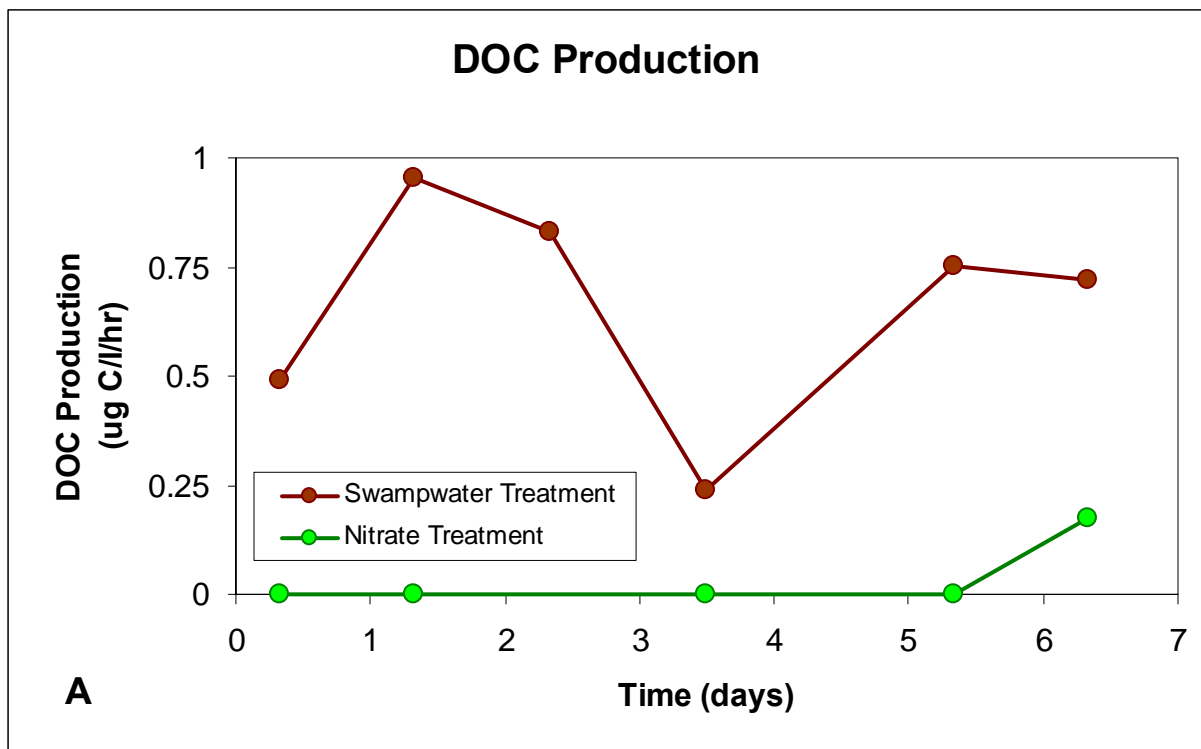


Figure 6 – Gross Primary Production. (A) DOC Production. (B) Biomass production. Note differences in scale.

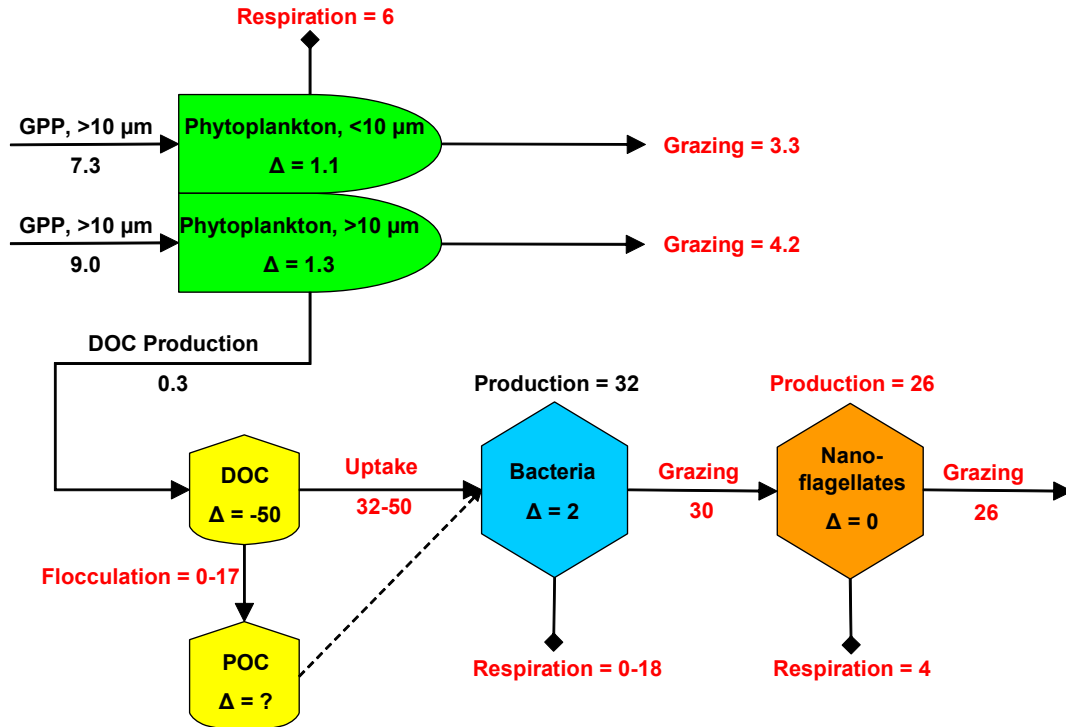


Figure 7 – Estimated carbon budget for microplankton in swampwater treatment. All values in $\mu\text{g C/l-hr}$. Black figures represent values measured directly. Red figures represent estimated/calculated values.

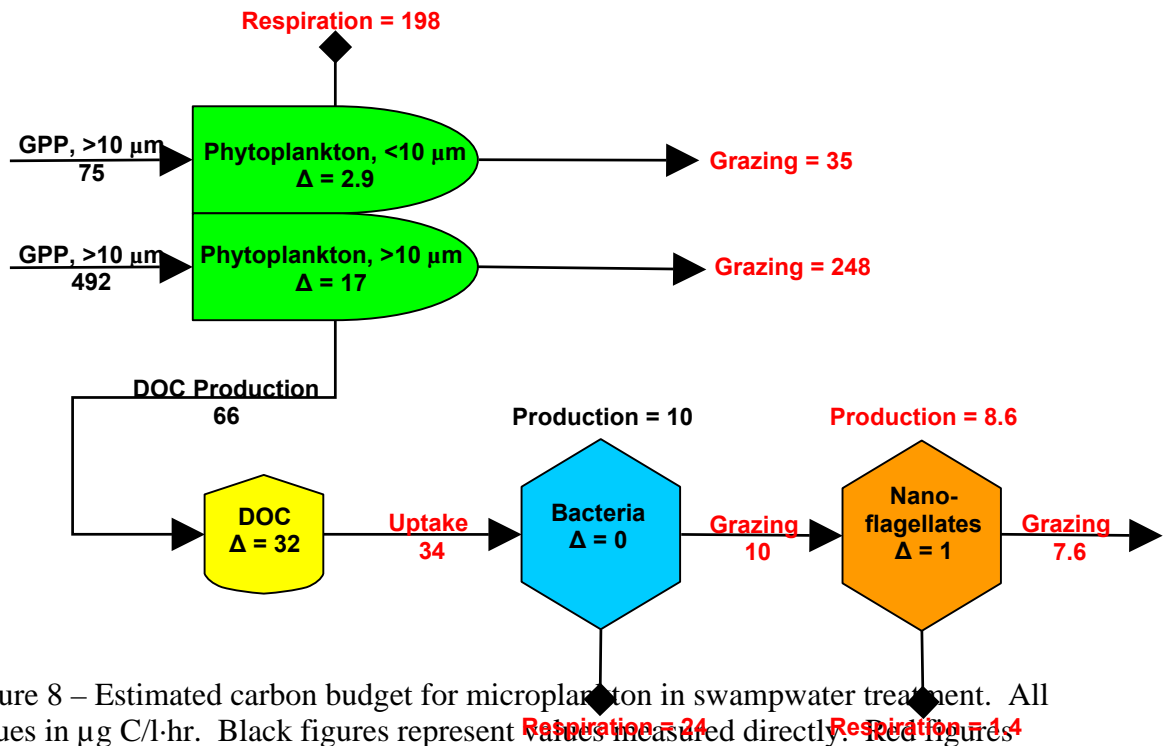


Figure 8 – Estimated carbon budget for microplankton in swampwater treatment. All values in $\mu\text{g C/l-hr}$. Black figures represent values measured directly. Red figures represent estimated/calculated values.